A project for a new alkali vapour magnetometer, optically pumped by a diode laser

Nicolò Beverini([1])([3]), **Osvaldo Faggioni**([2])([3]), **Cosmo Carmisciano**([3]), **Elena Alzetta**([1]), **Enrico Maccioni**([1]), **Mario Francesconi**([1]), **Alessandro Donati**([4]), **Emilio Simeone**([4]) **and Franco Strumia**([1])

([1]) *Dipartimento di Fisica dell'Università di Pisa and INFM, Unità di Pisa, Italy*

([2]) *Dipartimento di Scienze della Terra dell'Università di Pisa, Italy*

([3]) *Istituto di Geofisica e Ambiente Marino, Consorzio Universitario della Spezia, Italy*

([4]) *Kayser Italia s.r.l., Livorno, Italy*

Abstract

We present here a project for the industrial development of a new magnetometer that is intended to achieve the highest performance in measuring geomagnetic field. The instrument is based on the well-known technology of optically pumped alkali vapour magnetometers. Unlike current commercial models, a diode laser replaces the traditional radio-frequency lamp as pumping source and our magnetometer uses potassium as reference atom, contrary to the more traditional cesium or rubidium. The advantages of this choice are discussed. Preliminary experimental results on a prototype show an expected accuracy better than 1 $pT/Hz^{-1/2}$.

Key words *magnetometer – potassium – diode lasers*

1. The optically pumped alkali vapour magnetometers

An atomic magnetometer gives the absolute value of the intensity of the local magnetic field by measuring the frequency of the transition between two Zeeman sublevels of a paramagnetic atom. This transition can be observed with a very high signal-to-noise ratio, also in a very low density vapour (a few 10^{11} cm^{-3}) by using the method of optical pumping (Kastler, 1950). Let us irradiate an alkaline vapour by a monochromatic light beam, resonant with the D_1 optical transition between the ground state and the first excited level $^2P_{1/2}$. If the light is circularly polarised in the direction of the local magnetic field, only the atoms in the $m_z = -1/2$ sublevel can absorb the radiation. After a few absorption cycles the atoms are *optically pumped* into the non-absorbing $m_z = +1/2$ level, and the sample becomes transparent. The sample absorbs again when an *rf* field, resonant with the $m_z = -1/2 \leftrightarrow m_z = +1/2$ transition, repopulates the $m_z = -1/2$ level. Thus, a change in the transmission of one optical photon corresponds to every absorbed rf photon, with a gain equal to the ratio between the energy of the optical and the rf photon ($\approx 10^9$!).

The actual operating schemes for measuring the Zeeman resonance frequency are essentially two (Bell and Bloom, 1957). In the first one (*locked magnetometer* or M_z *magnetometer*, fig. 1), the atomic sample is optically pumped in the direction of the static magnetic field (z-direction), and a Voltage Controlled

Mailing address: Dr. Nicolò Beverini, Dipartimento di Fisica dell'Università di Pisa, Via F. Buonarroti 2, 56126 Pisa, Italy; e-mail: beverini@mailbox.difi.unipi.it

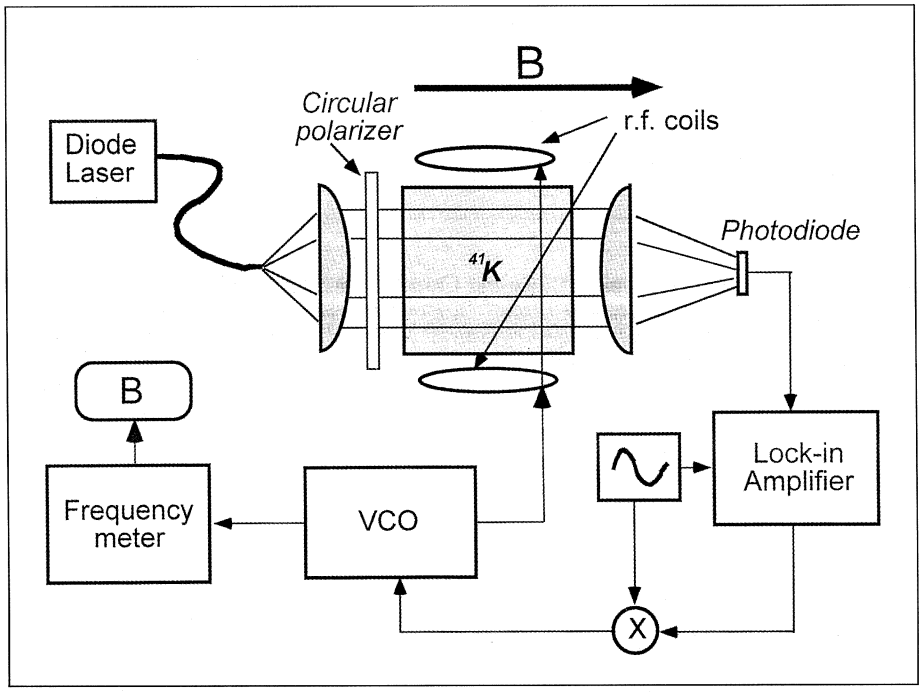

Fig. 1. Locked (M_z) magnetometer.

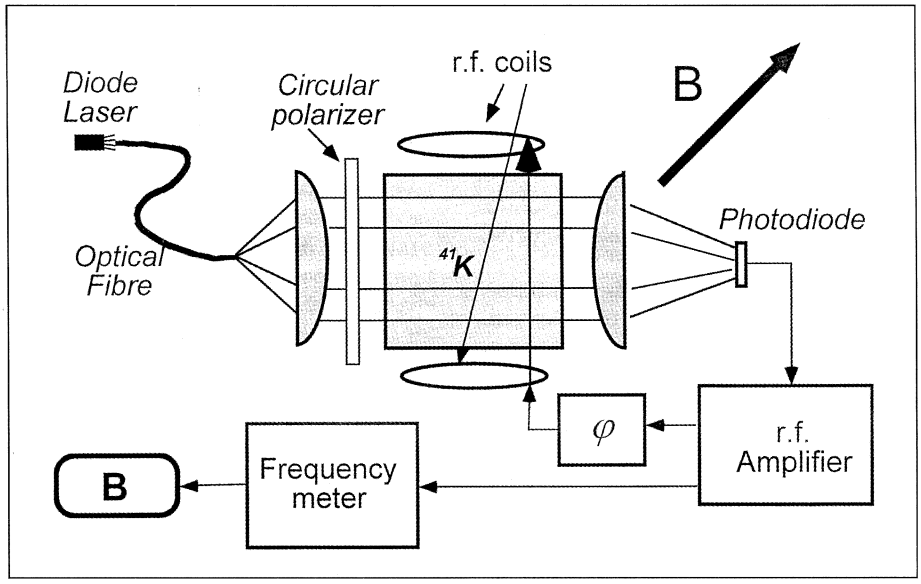

Fig. 2. Self-oscillating (M_x) magnetometer.

Oscillator (VCO) is phase-locked to the transition.

In the second scheme (*self-oscillating magnetometer* or M_x *magnetometer*, fig. 2), the circular polarised optical radiation is sent on the atomic sample in a direction transverse to the static magnetic field (at an angle of about 45°). An atom, which is initially oriented by the light in the transverse direction, then precedes around the field at the Larmor frequency. If the precession of the oriented atoms is driven in phase by a resonant rf field, a macroscopic rotating magnetic moment is generated, that modulates the atomic sample transmission. A self-oscillating system at the Larmor frequency is thus generated by sending the amplified photodiode signal in positive feed-back on the rf coils.

The first scheme is intrinsically more accurate, but its acquisition speed is limited by the presence of the low-frequency modulation, that should be slower than the physical system response time and consequently of the order of some Hz, and requires a more complex electronics. In the second one, the flatness of the phase response in the feed-back loop is critical in order to avoid spurious frequency shifts, but it is almost universally preferred for its simplicity and its fast response time.

A third scheme is also possible, in which no rf field is applied to the cell while the light source is modulated in amplitude at the resonance frequency (Bell and Bloom, 1961). The diode lasers that we use as pumping source can be easily modulated on/off at the required frequencies. This scheme suffers, however, from a theoretical signal-to-noise ratio a factor 2 lower than in the other two cases.

2. The potassium vapour magnetometer

The above description of an alkali magnetometer neglects the interaction between the electronic spin and the magnetic moment associated with the nuclear spin I. At zero magnetic field, the ground state splits in two hyperfine levels, defined by the value of the total angular momentum $F = I \pm 1/2$. When an external magnetic field B removes the degeneration between the Zeeman components, the transition frequencies are calculated from the Breit-Rabi formula

$$\nu_{F,\, m_F \to F,\, m_F - 1} = g_I \frac{\mu_B}{h} B + \tag{2.1}$$

$$+ \frac{W}{2}\left[\sqrt{1 + \frac{4m_F}{2I+1}x + x^2} - \sqrt{1 + \frac{4(m_F-1)}{2I+1}x + x^2}\right]$$

where W is the hyperfine frequency separation, g_I is the nuclear Landé factor, μ_B is Bohr's magneton, and $x = (g_J - g_I)\,\mu_B B/hW$.

Equation (2.1) can be expanded in series of powers as

$$\nu_{F,\, m_F \to F,\, m_F - 1} = \tag{2.2}$$

$$= \gamma_F B + \alpha_m^{(2)} \cdot \gamma^{(2)} B^2 + \alpha_m^{(3)} \cdot \gamma^{(3)} B^3 + \ldots$$

where

$$\gamma_F = \frac{\mu_B}{h}[(g_J - g_I)/(2I+1) + g_I],$$

$$\gamma^{(2)} = \frac{1}{W}\left(\frac{\mu_B}{h}\frac{g_J - g_I}{2I+1}\right)^2,$$

$$\gamma^{(3)} = \frac{1}{W^2}\left(\frac{\mu_B}{h}\frac{g_J - g_I}{2I+1}\right)^3,$$

$$\alpha_m^{(2)} = (1 - 2m_F),$$

$$\alpha_m^{(3)} = 2\,(1 - 3m_F + 3m_F^2) - \frac{1}{2}(2I+1)^2.$$

The most important parameters for the naturally available isotopes of Cs, Rb and K are reported in table I.

The presence of non-linear terms produces a slight difference between the frequencies of the Zeeman transitions. Cesium has the largest hyperfine structure, and consequently the smallest $\gamma^{(2)}$ factor, while the contrary appears to the two potassium isotopes. At a typical earth field level ($B \approx 50\,000$ nT), the separation between two nearby transitions is 6.67 Hz and 958.3 Hz in the case of Cs and ^{41}K, respectively.

Table I. Physical parameters for the naturally available isotopes of Cs, Rb and K.

	Cs	^{85}Rb	^{87}Rb	^{39}K	^{41}K
I	7/2	5/2	3/2	3/2	3/2
W (MHz)	9192.631770	3035.732439	6834.682613	461.7197202	254.013871
g_J	2.00254032	2.00233113	2.00233113	2.00229421	2.00229421
g_I	$-3.9885395 \cdot 10^{-4}$	$-2.936400 \cdot 10^{-4}$	$-9.951414 \cdot 10^{-4}$	$-1.4193489 \cdot 10^{-4}$	$-0.779060 \cdot 10^{-4}$
γ_F (Hz/T)	$3.49862 \cdot 10^9$	$4.66743 \cdot 10^9$	$6.99583 \cdot 10^9$	$7.00466 \cdot 10^9$	$7.00533 \cdot 10^9$
$\gamma^{(2)}$(Hz/T^2)	$1.33579 \cdot 10^9$	$7.18879 \cdot 10^9$	$7.18932 \cdot 10^9$	$1.06327 \cdot 10^{11}$	$1.93257 \cdot 10^{11}$

By using resonant circularly polarised σ^+ (σ^-) radiation, the atoms are optically pumped in the sublevel that has the highest (lowest) m_F value, and the Zeeman transition leaving from this sublevel would be the only one observable. Unfortunately, the unavoidable relaxation processes also make observable the other transitions. The typical linewidth of the Zeeman transitions in a magnetometer is in the range 10-100 Hz, and thus for Cs the different transitions overlap, producing a non-symmetrical profile with the peak shifted in frequency. The relative weight of the different transitions is a complex function of all the physical conditions of the magnetometer (temperature of the vessel, intensity of the radiation source, relative alignment of the magnetometer and the local field, ...), this effect is the source of relative large errors, of the order of 10 nT or more. Skilled design of the magnetometer compensates this asymmetry by combining the signals of two apparatus acting with opposite polarisation (Yabuzaki and Ogawa, 1974). This scheme is applied to the commercial Cs magnetometers. The exact balance between the two signals is however critical. The accuracy of the instrument is then easily affected by the physical environment conditions, and is usually limited to about 1 nT, while the sensitivity can be up to three orders of magnitude better.

The traditional source for the pumping optical radiation was the low pressure spectral lamp, excited by an rf discharge. These lamps are quite efficient and reliable in the case of Cs and Rb, but not for K, because its vapour attacks and darkens ordinary glass, reducing the lifetime of the lamp. Moreover, the spectrum of an alkali atom presents near the D_1 line, connecting the ground state with the $^2P_{1/2}$ level, a second line D_2, connecting the ground state with the $^2P_{3/2}$ level. D_1 or D_2 lines pump the vapour in opposite directions, and it is necessary to filter out one line. This filtering is easy for Cs and Rb, but rather difficult for K (the difference between D_1 and D_2 wavelengths are 42 nm, 15 nm, and 3 nm respectively).

3. Our diode laser pumped prototype

The construction of a prototype of optically pumped potassium magnetometer is underway with the purpose of future industrial development. The use of a single mode diode laser as pumping source overcomes the difficulties connected with potassium spectral lamps.

The first tests were made by using as probe a sealed off Pyrex cell, 25 mm in length and 22 mm in diameter, filled with natural potassium (91% ^{39}K and 9% ^{41}K) under vacuum distillation, and nitrogen as buffer gas at a pressure of about 6.5 kPa (at 0 °C). The diffusion in a diamagnetic buffer gas avoids a fast relaxation of the atomic orientation against the vessel walls. We measured a relaxation time of $\approx$ 100 ms at the working temperature of our cell ($\approx$ 80° C). Nitrogen is also very effective in quenching the fluorescence from the excited K atoms, thus avoiding the presence of resonance radiation, that could perturb the pumping process. The presence of the buffer gas also increases the optical pumping efficiency, by

broadening the homogeneous optical absorption linewidth. We calculate a pressure broadening in our cell of about 680 MHz (Allard and Kielkopf, 1982), that is of the same order of the hyperfine structure and of the Doppler thermal linewidth. The absorption line is thus homogeneous, and every atom can interact with the radiation, independently of its velocity and hyperfine level.

Figure 3 shows the lineshape of the resonance, as recorded by pumping the probe cell with radiation circularly polarised in the direction of the local magnetic field. The light transmitted by the K cell is detected, while the frequency of the applied ac field is tuned across the Zeeman resonance. The pumping power is about 10 μW, while rf power is about -55 dBm. The absorption signal (at left) shows the well resolved different Zeeman components of ^{39}K and ^{41}K. The derivative signal (at right), recorded using a frequency modulation technique and in-phase detection, evidences a resonance linewidth $\Delta\nu$ of 75 Hz, with a signal-to-noise ratio S/N of the order of 300. Further work is in progress to build a magnetometer in the M_x scheme, using isotopically enriched sample of ^{41}K. The optical fibre delivery of the radiation from the laser to the probe currently limits the S/N ratio. A new transmission system, more stable mechanically, and the use of a larger potassium cell ($\approx$ 4 cm) will reduce the noise and the linewidth $\Delta\nu$. Making the conservative assumption of achieving a linewidth $\Delta\nu = 20$ Hz and S/N $\approx$ 1000 (in 1 Hz bandwidth), we can calculate an expected precision in the frequency measurement $\delta\nu = \Delta\nu/(2 \cdot \mathrm{S/N})$, and thus an instrumental sensitivity $(\delta B)_{\min} \approx \delta\nu/\gamma = 1.3\ \mathrm{pT} \cdot \mathrm{Hz}^{-1/2}$.

This performance is competitive with top-class commercial Cs magnetometers. Also the dimension and the final cost of the apparatus would be comparable. As we stated above, in the case of potassium the reference is a single well resolved Zeeman component, unlike the case of cesium. This makes the instrument much less sensitive to the environment, and

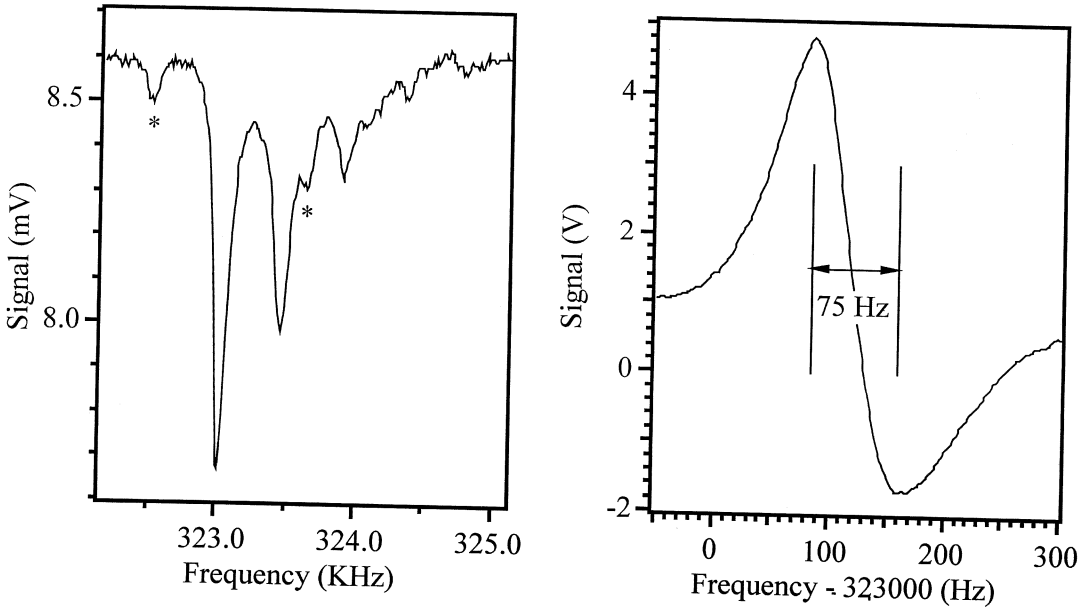

Fig. 3. Natural potassium resonance signal. At left: the full Zeeman spectrum (* labels ^{41}K transitions); the magnetic field was 46 210 nT. At right: the ^{39}K $F = 2$, m_F 2 $\rightarrow$ 1 transition observed through the lock-in amplifier.

then intrinsically more accurate, especially in mobile apparatus. Diode lasers have high plug-in electrical efficiency and require less power than rf spectral lamps, have better spectral properties and a very low amplitude noise. Their radiation can be easily delivered in optical fibres, and it is possible to separate physically the electronic apparatus, radiation source included, from the probe, removing eventual perturbation. The high accuracy of the instrument makes it especially suitable for gradiometric application, where a single diode laser may be used to pump more probes, reducing the systematic errors.

REFERENCES

KASTLER, A. (1950): Prodution et détection optique d'une inégalité de population, *J. Phys. Rad.*, **11**, 255-265.

BELL, W.E. and A.L. BLOOM (1957): Optical detection of magnetic resonance, *Phys. Rev.*, **107**, 1559-1565.

BELL, W.E. and A.L. BLOOM (1961): Observation of forbidden resonances in optically driven spin systems, *Phys. Rev. Lett.*, **6**, 623-624.

YABUZAKI, T. and T. OGAWA, (1974): Frequency shifts of self-oscillating magnetometer with cesium vapor, *J. Appl. Phys.*, **45**, 1342-1355.

ALLARD, N. and J. KIELKOPF (1982): The effect of neutral nonresonant collisions on atomic spectral lines, *Rev. Mod. Phys.*, **54**, 1103-1182.